JACS
JOURNAL OF THE AMERICAN CHEMICAL SOCIETY

Communication

pubs.acs.org/JACS

Shock-Induced Ordering in a Nano-segregated Network-Forming Ionic Liquid

Ke Yang,[†,§,⊥] Jaejun Lee,[†,§,⊥] Nancy R. Sottos,[†,§] and Jeffrey S. Moore*[,†,‡,§]

[†]Department of Materials Science and Engineering, [‡]Department of Chemistry, and [§]Beckman Institute for Advanced Science and Technology, University of Illinois at Urbana−Champaign, Urbana, Illinois 61801, United States

Supporting Information

ABSTRACT: Understanding shockwave-induced physical and chemical changes of impact-absorbing materials is an important step toward the rational design of materials that mitigate the damage. In this work, we report a series of network-forming ionic liquids (NILs) that possess an intriguing shockwave absorption property upon laser-induced shockwave. Microstructure analysis by X-ray scattering suggests nano-segregation of alkyl side chains and charged head groups in NILs. Further post-shock observations indicate changes in the low-Q region, implying that the soft alkyl domain in NILs plays an important role in absorbing shockwaves. Interestingly, we observe a shock-induced ordering in the NIL with the longest (hexyl) side chain, indicating that both nano-segregated structure and shock-induced ordering contribute to NIL's shockwave absorption performance.

Shockwave dissipation materials function to protect personnel and structures from blast overpressure. During shockwave propagation, the brain is especially susceptible to shockwave overpressure. Previous studies have revealed that when brain tissues are exposed to high-intensity shockwaves >10 MPa, severe hemorrhage is possible. Exposure to low-intensity shockwaves <1 MPa also causes minor morphological changes in neurons, leading to mild-to-moderate traumatic brain injury (mTBI).[1] The human resource loss from mTBI has a significant direct economic impact along with indirect costs due to loss of earning ability and the burden of care.[2] Therefore, there are urgent needs to develop materials that effectively absorb low-intensity shockwaves.

Polyurea (PU) is the benchmark material that exhibits effective shockwave absorption properties. Despite >5 years of study, the mechanism by which PU absorbs shockwaves is still under debate.[3] Both experimental data and computational models (mesoscale, all-atom, and coarse-grained molecular level) have offered insights into PU's shockwave attenuation capability.[4] Roland et al. suggested that hydrogen-bond-abundant, hard domains of PU have a small or negligible role in shockwave absorption.[5] Grujicic et al. confirmed that the impact-induced rubbery-to-glassy transition acts as a potent ballistic-resistance-enhancing mechanism but not a shock-mitigating mechanism.[6] In addition, Grujicic et al. stated that shock-induced H-bond-breaking in hard domains plays an important role in the shock-impact mitigation capacity of PU.[4a] They also proposed shock-induced ordering within the hard domains and viscoelastic relaxation within the hard/soft interfacial regions as another mechanism for reducing shock impact.[7] Even though an explicit shockwave absorption mechanism is absent, these groups along with other researchers reached the agreement that the micro-phase segregation in PU plays an important role in its high shockwave absorption performance.

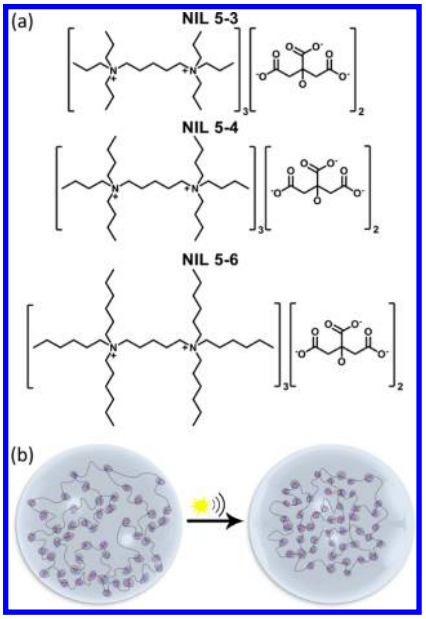

Figure 1. (a) Chemical scheme for the network-forming ionic liquids (NILs) under investigation. These ionic liquids are named as "NIL #A-#B", where #A is the backbone methylene unit number and #B is the side-chain methylene/methyl unit number. (b) Schematic depiction of shock-induced ordering in nano-segregated NIL. The clusters represent the charged head groups, and the connection lines represent the inter-connected soft alkyl domains.

Similar to the micro-phase segregation observed in PU, amphiphilic ionic liquids (ILs) with alkyl tails also display structural heterogeneities on the nanometer spatial scale that may make them effective candidates for shockwave energy dissipation.[8] Evidence from both computer simulation and neutron/X-ray diffraction suggested that the alkyl chains in ILs pack into a "soft, oily" matrix, while the charged head groups tend to segregate into "hard" domains.[9] Recently, Yang et al.

Received: October 13, 2015
Published: December 10, 2015

DOI: 10.1021/jacs.5b10721
J. Am. Chem. Soc. 2015, 137, 16000−16003

studied a class of network-forming ionic liquids (NILs, see Figure 1) composed of alkyl-diammonium cations and citrate anions.[10] The long alkyl side chains of the cations are used to frustrate the crystallization so that amorphous glassy solids form upon cooling. Peaks in the low-Q(scattering vector) ($Q \approx 0.4-0.7$ Å^{-1}) regime, corresponding to the nanometer spatial scale, provide the signature of structural heterogeneities in NILs.

Laser-induced stress waves are used to characterize the shockwave absorption property of NILs. As shown schematically in Figure 2, shockwaves are generated by impingement of

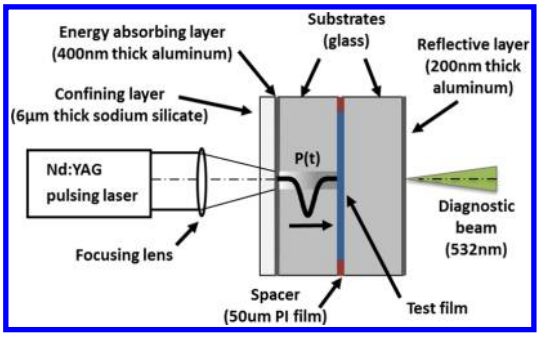

Figure 2. Schematic depiction of laser-induced shockwave experimental test setup and specimen structure.

a high-energy Nd:YAG pulsed laser on a 400 nm thick Al energy-absorbing layer.[11] Transfer of energy from the laser pulse leads to rapid expansion of the Al layer. The presence of the confining layer on top of the Al film causes a high-amplitude compressive shockwave to propagate through the specimen. The YAG laser power and beam diameter were varied to systematically control the laser fluence. The out-of-plane displacement of the specimen's surface was measured using a Michelson interferometer with a 532 nm laser diagnostic beam. A photodetector connected to 40 GHz oscilloscope recorded the interference signal, which was converted to displacement and velocity history (as described previously by Wang et al.[11a]). The pressure profile, $P(t)$, was obtained from the velocity history using conservation of momentum,

$$P(t) = \rho_0(U_s(t))U_p(t) = \rho_0(s + cU_p(t))U_p(t) \quad (1)$$

where ρ_0 is the initial material density and $U_p(t)$ is the particle velocity obtained from the measurement. Shock velocity, $U_s(t)$, is given by $s + cU_p(t)$, where s and c are fitted parameters from the U_s-U_p Hugoniot relation of the substrate. The energy per area, i.e., total transmitted energy, was calculated from the velocity history using conservation of energy and momentum as previously described by Forbes,[12]

$$J(t) = \frac{1}{2}\rho_0 \int_0^t (U_p(t))^2(s + cU_p(t))\, dt \quad (2)$$

Interferometric data under the shockwave impact were recorded for all NIL samples using PU as a reference (Figure S1 in the Supporting Information (SI)).[11a,f] The NIL test specimens were prepared by sandwiching a 50 μm thin film between two glass substrates (a detailed description of specimen preparation is given in the SI). The pressure profiles and total transferred shockwave energy were calculated from the measured surface velocity using eqs 1 and 2. Input pressure profiles were obtained from specimens prepared without a test

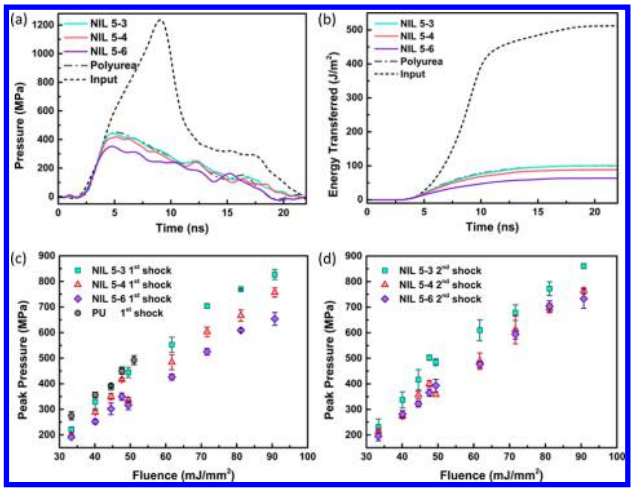

Figure 3. (a) Representative pressure profiles of NIL samples and PU obtained during laser-induced shockwave test at 48 mJ/mm^2 laser fluence. (b) Representative total transferred energy profiles of NIL and benchmark PU specimens at 48 mJ/mm^2 laser fluence. (c) Average peak pressures at different laser fluences for pristine samples including PU. (d) Average peak pressures at different laser fluences for post-shock NIL samples. Error bars represent standard error.

film, as described in Figure S2 in the SI. Shockwave loading resulted in a characteristic pressure profile displaying an abrupt rise on the nanosecond time scale. Representative pressure profiles for the different NILs are compared to the input and the benchmark PU pressure profiles at 48 mJ/mm^2 laser fluence in Figure 3a. All of the materials tested caused a desirable reduction in peak pressure. As shown in Figure 3a, the absorption of shockwave energy by NILs and PU also resulted in a shift of peak pressure over time. The total transferred energy is plotted in Figure 3b. NIL 5-4 and NIL 5-6 dissipated 82.7% and 87.6% of the total input energy at 48 mJ/mm^2 fluence, respectively. Both the reduction in peak pressure and the reduction in total energy demonstrate that NILs are effective shockwave absorption materials. In addition, the NILs with longer side chains exhibited superior shockwave absorption performance. Average peak pressures of pristine NILs and PU obtained from multiple pressure profile data at each laser fluence are plotted in Figure 3c. The NILs with longer alkyl chains attenuated more shockwave peak pressure than NILs with shorter alkyl chains at all fluences.

To determine whether the NILs were capable of absorbing multiple rounds of shockwave impact, we measured the shockwave absorption of post-shock NILs at various laser fluences (Figure 3d). Peak pressures obtained from pristine and post-shock NILs correspond to those from first-shock and second-shock NILs in Figure 3c,d. The peak pressure of the post-shock sample was measured following a single shockwave impact, i.e., first shock, on pristine NILs. The experimental procedure for measuring shockwave absorption properties of pristine and post-shock NILs is described in the SI. Plotting the average peak pressures of all pristine NIL samples against laser fluences revealed that the shockwave energy dissipation performance of NIL 5-6 is the best in the series, followed by NIL 5-4, NIL 5-3, and PU at all input fluences (Figure 3c). Furthermore, the peak pressure differences between NILs increased with fluence since higher input laser fluences generated stronger shockwaves. For the post-shock NILs samples, the peak pressures of NIL 5-3 and NIL 5-4 remained unchanged compared to the peak pressures from pristine

DOI: 10.1021/jacs.5b10721
J. Am. Chem. Soc. 2015, 137, 16000−16003

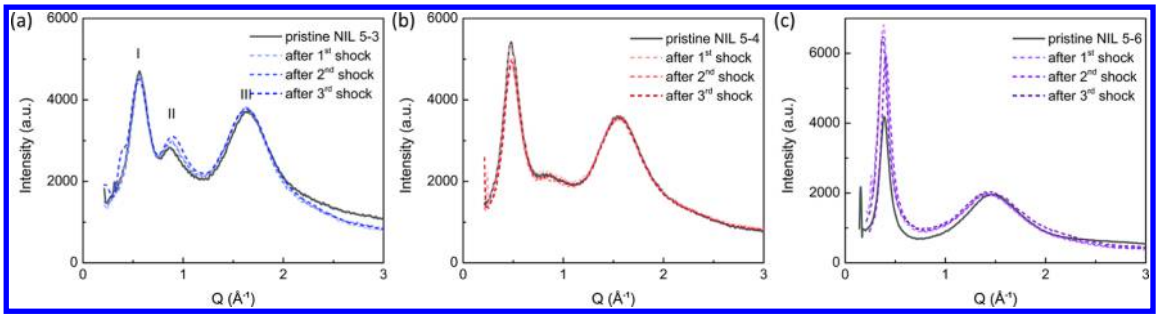

Figure 4. XRD patterns before and after shockwave impact for samples (a) NIL 5-3, (b) NIL 5-4, and (c) NIL 5-6. For NIL 5-3 and NIL 5-4, multiple shockwave impacts did not change the microstructure significantly, while for NIL 5-6, the amplitude of the low-Q peak (peak I) increased significantly.

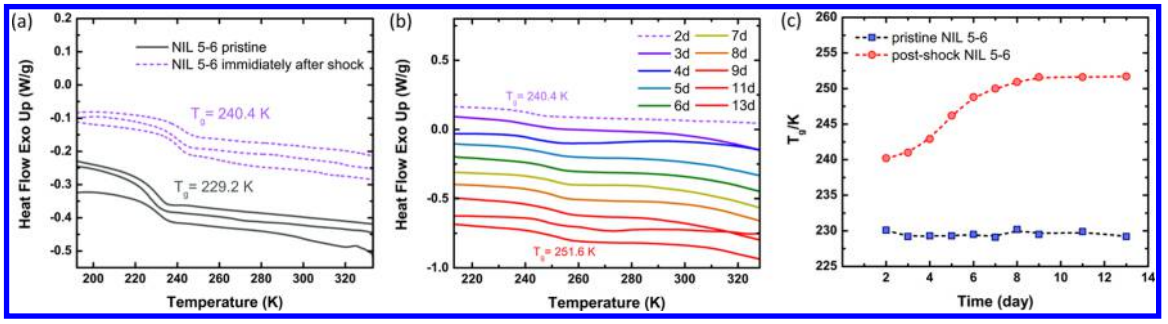

Figure 5. (a) Differential scanning calorimetry (DSC) measurements of three batches of NIL 5-6 pristine samples and post-shock samples. Glass transition temperature (T_g) value is marked. (b) DSC curves' time evolution for post-shock NIL 5-6 samples. Over 7 days at room temperature, the T_g of post-shock samples increased by 11.2 K. From day 7 to day 11, T_g did not change. (c) Plot of T_g as a function of time for pristine NIL 5-6 sample and post-shock sample. The 0 day point is when samples were freshly prepared. The samples were freeze-dried for 2 days prior to DSC measurements and shock impacts.

samples. In contrast, the peak pressure of post-shock NIL 5-6 increased and became comparable to that of NIL 5-4. Given that NIL 5-6 lost shockwave absorption ability after the first shockwave impact, we hypothesized that pristine NIL 5-6 attenuated the impact via a slow relaxation or an irreversible alteration of material structure.

Powder X-ray diffraction (PXRD) enables microstructural analyses of pristine and post-shock NILs, thereby offering insights into NILs' shockwave attenuation mechanism (Figure 4). PXRD patterns of all NIL samples reflect their amorphous nature. There are three major diffraction features in the XRD plots. With a rough calculation based on the Q value at each peak's position, the correlation lengths for features resulting in peaks I, II, and III are 11−13, 7−8, and 3.8−4.4 Å, respectively. In particular, peak I has been observed in various IL systems, including alkyl-ammonium/phosphonium-based salts, imidazolium salts, and other protic ILs, and detailed neutron and X-ray scattering data show that it represents features associated with the structural heterogeneities on the nanometer spatial scale.[9b] A previous study also demonstrated that even short alkyl chains, such as ethyl or propyl groups, cause such heterogeneity.[9a] The solvophobic interaction between alkyl chains and charged heads likely plays an important role in leading to this structural heterogeneity. Moreover, as alkyl side-chain length increases, the nonpolar domains become interconnected and cause "swelling" of the entire ionic network, resulting in a "sponge-like" structure.[13] Comparing pristine samples of NIL 5-3 and NIL 5-6, it is evident that peak I in XRD shifts to lower Q values, indicating that the size of the heterogeneous domain increases. This result, along with the trend of shockwave dissipation, suggests that shockwave attenuation performance correlates positively with side-chain length. After multiple shock impacts (up to three), the XRD patterns of NILs 5-3 and 5-4 remain the same, indicating little change in the microstructure. In contrast, there is peak sharpening, with almost a 2-fold increase of the amplitude of peak I for NIL 5-6 after the initial impact, suggesting that the segregation related to peak I becomes better defined. Specifically, the polar atoms (especially anion−anion correlations) across intervening non-polar domains become better correlated. The unchanged peak position indicates that the shockwave impact does not affect the size of the domains. We propose that the shockwave causes the polar heads in NIL 5-6, which has the largest structural heterogeneity, to rearrange into a more correlated configuration. This rearrangement is responsible for the increase of NIL 5-6's peak pressure after first-shock impact.

To further validate the existence of hypothesized shock-induced ordering, we examined the differential scanning calorimetry (DSC) of pristine NIL 5-6 and re-recorded the DSC data immediately after shocking on pristine samples (Figure 5). Pristine NIL 5-6 has a glass transition temperature (T_g) of 229.2 K. After the first shock, the T_g of NIL 5-6 increased to 240.4 K. NMR and mass spectrometry on post-shock samples ruled out the possibility of any shock-induced chemical changes. These results are consistent with our hypothesis of shock-induced ordering in the heterogeneous domain. The 11.2 K increase of T_g may be due to the extra spatial hindrance from the more ordered heterogeneous domain. To examine whether this rearrangement relaxes after shockwave impact, we kept the post-shock NIL 5-6 sample at room temperature and recorded the DSC curves' time

DOI: 10.1021/jacs.5b10721
J. Am. Chem. Soc. 2015, 137, 16000−16003

evolution of the post-shock sample over a period of 11 days. The T_g of NIL 5-6 increased by another 11.2 K over 7 days and reached a stable value of 251.6 K. This result indicates that the ordering process continues for days after the shockwave impacts. The relaxation dynamics is rather slow due to the high viscosity of NILs at room temperature. For comparison, the T_g of pristine NIL 5-6 is rather stable for months at room temperature.

The energy landscape theory of amorphous materials provides a viewpoint to qualitatively explain our observations. We hypothesize that the spatial correlation of polar heads and non-polar alkyl chains can potentially be rearranged by overcoming an energy barrier. Similar effects have been observed under high hydrostatic pressures. For example, high pressure can cause configurational changes in the alkyl groups of imidazolium ILs.[14] Apparently, NILs with longer alkyl chains, such as NIL 5-6, are more easily reorganized because there is less restriction from the charged headgroup. The major structural change occurs at the first shock impact because the more correlated conformations are more stable. We also hypothesize that the molecular conformation does not reach its local energy minimum immediately after the shockwave impacts, so the ordering process slowly continues over time. To the best of our knowledge, this is the first time that shock-induced ordering in the liquid phase has been observed. With higher shockwave energy, further configurational changes of NIL along its energy landscape may occur, including possible formation of a crystal or ideal glass.

Combining these findings with the multiple-shock experiments, the relationship between the microstructures of NILs and their shockwave absorption performances is evident. In NIL 5-3 and NIL 5-4, the microstructure and shockwave absorption performance do not change through multiple shocks. In NIL 5-6, subsequent shockwave absorption performance is reduced by irreversible shock-induced structural evolution and ordering in nano-segregated domains from the first shockwave impact. We conclude that the observed shock-induced ordering contributes to the better shockwave absorption performance in the initial shock of NIL 5-6. Thus, at least two mechanisms of shockwave absorption exist in the NIL system. First, in the cases of NIL 5-3 and NIL 5-4, the nano-segregated ionic network in the NIL dissipates shockwave kinetic energy without causing noticeable structural change. In addition, in the case of NIL 5-6, an irreversible change in spatial ordering within the ionic network also plays a key role in extra shockwave energy-absorbing capability.

In summary, the current study introduces a new class of shockwave absorption materials, based on shockwave-induced microstructural changes in NILs. We observe a shock-induced ordering that depends on the chain length of the soft alkyl domain of the NIL. Both the nano-segregated morphology and shock-induced ordering process contribute to the shockwave performance of the NILs. Incorporating these approaches into shockwave absorption systems will provide new insights in the field. The effects of other parameters, such as ion charge density, backbone chain length, degree of nano-segregation, and size of hard/soft domain, on the shockwave absorption performance will be investigated in due course.

■ ASSOCIATED CONTENT

Supporting Information

The Supporting Information is available free of charge on the ACS Publications website at DOI: 10.1021/jacs.5b10721.

Syntheses and details of the shockwave test, XRD, and DSC measurements (PDF)

■ AUTHOR INFORMATION

Corresponding Author

*jsmoore@illinois.edu

Author Contributions

⊥K.Y. and J.L. contributed equally.

Notes

The authors declare no competing financial interest.

■ ACKNOWLEDGMENTS

We acknowledge financial support from the Department of the Navy, Office of Naval Research, Grant No. 0014-12-1-0828.

■ REFERENCES

(1) Nakagawa, A.; Manley, G. T.; Gean, A. D.; Ohtani, K.; Armonda, R.; Tsukamoto, A.; Yamamoto, H.; Takayama, K.; Tominaga, T. *J. Neurotrauma* **2011**, *28*, 1101−1119.

(2) Courtney, A. C.; Courtney, M. W. *Med. Hypotheses* **2009**, *72*, 76−83.

(3) (a) Bahei-El-Din, Y. A.; Dvorak, G. J.; Fredricksen, O. J. *Int. J. Solids Struct.* **2006**, *43*, 7644−7658. (b) Grujicic, A.; LaBerge, M.; Grujicic, M.; Pandurangan, B.; Runt, J.; Tarter, J.; Dillon, G. *J. Mater. Eng. Perform.* **2012**, *21*, 1562−1579. (c) Gardner, N.; Wang, E.; Kumar, P.; Shukla, A. *Exp. Mech.* **2012**, *52*, 119−133.

(4) (a) Grujicic, M.; Pandurangan, B.; Bell, W. C.; Cheeseman, B. A.; Yen, C.-F.; Randow, C. L. *Mater. Sci. Eng., A* **2011**, *528*, 3799−3808. (b) Grujicic, M.; Pandurangan, B. *J. Mater. Sci.* **2012**, *47*, 3876−3889. (c) Arman, B.; Reddy, A. S.; Arya, G. *Macromolecules* **2012**, *45*, 3247−3255.

(5) Bogoslovov, R. B.; Roland, C. M.; Gamache, R. M. *Appl. Phys. Lett.* **2007**, *90*, 221910.

(6) Grujicic, M.; Pandurangan, B.; He, T.; Cheeseman, B. A.; Yen, C.-F.; Randow, C. L. *Mater. Sci. Eng., A* **2010**, *527*, 7741−7751.

(7) Grujicic, M.; Snipes, J. S.; Ramaswami, S.; Yavari, R.; Runt, J.; Tarter, J.; Dillon, G. *J. Mater. Eng. Perform.* **2013**, *22*, 1964−1981.

(8) (a) Zhao, Y.; Hu, Z. *Chem. Commun.* **2012**, *48*, 2231−2233. (b) Song, X.; Hamano, H.; Minofar, B.; et al. *J. Phys. Chem. B* **2012**, *116*, 2801−2813. (c) Ji, Y.; Shi, R.; Wang, Y.; Saielli, G. *J. Phys. Chem. B* **2013**, *117*, 1104−1109. (d) Canongia Lopes, J. N. A.; Pádua, A. A. H. *J. Phys. Chem. B* **2006**, *110*, 3330−3335. (e) Hettige, J. J.; Araque, J. C.; Margulis, C. J. *J. Phys. Chem. B* **2014**, *118*, 12706−12716. (f) Li, S.; Bañuelos, J. L.; Zhang, P.; Feng, G.; Dai, S.; Rother, G.; Cummings, P. T. *Soft Matter* **2014**, *10*, 9193−9200.

(9) (a) Atkin, R.; Warr, G. G. *J. Phys. Chem. B* **2008**, *112*, 4164−4166. (b) Zheng, W.; Mohammed, A.; Hines, L. G.; et al. *J. Phys. Chem. B* **2011**, *115*, 6572−6584.

(10) Yang, K.; Tyagi, M.; Moore, J. S.; Zhang, Y. *J. Am. Chem. Soc.* **2014**, *136*, 1268−1271.

(11) (a) Wang, J.; Weaver, R. L.; Sottos, N. R. *Exp. Mech.* **2002**, *42*, 74−83. (b) Grady, M. E.; Geubelle, P. H.; Braun, P. V.; Sottos, N. R. *Langmuir* **2014**, *30*, 11096−11102. (c) Grady, M. E.; Beiermann, B. A.; Moore, J. S.; Sottos, N. R. *ACS Appl. Mater. Interfaces* **2014**, *6*, 5350−5355. (d) Youssef, G.; Gupta, V. *Exp. Mech.* **2013**, *53*, 145−154. (e) Youssef, G.; Gupta, V. *Mech. Time-Depend. Mater.* **2012**, *16*, 317−328. (f) Gupta, V.; Argon, A. S.; Parks, D. M.; Cornie, J. A. *J. Mech. Phys. Solids* **1992**, *40*, 141−180.

(12) Forbes, J. W. *Shock Wave Compression of Condensed Matter*; Springer: Berlin, 2012; pp 13−29.

(13) Hayes, R.; Imberti, S.; Warr, G. G.; Atkin, R. *Phys. Chem. Chem. Phys.* **2011**, *13*, 13544−13551.

(14) (a) Zhao, Y.; Liu, X.; Lu, X.; et al. *J. Phys. Chem. B* **2012**, *116*, 10876−10884. (b) Gardas, R. L.; Freire, M. G.; Carvalho, P. J.; Marrucho, I. M.; Fonseca, I. M. A.; Ferreira, A. G. M.; Coutinho, J. A. P. *J. Chem. Eng. Data* **2007**, *52*, 80−88.

DOI: 10.1021/jacs.5b10721
J. Am. Chem. Soc. 2015, 137, 16000−16003